Electronic Supplementary Material (ESI) for RSC Advances.

From oxides to oxysulfides: mixed-anion GeS_3O unit induces the huge improvement on nonlinear optical effect and optical anisotropy as potential nonlinear optical materials

Xinyu Tian‡, Xiaodong Zhang,‡ Yan Xiao‡, Xiaowen Wu*, Bingbing Zhang, Daqing Yang, Kui Wu*

College of Chemistry and Environmental Science, Hebei University, Baoding, China

To whom correspondence should be addressed :

E-mail: wukui@hbu.edu.cn (Kui Wu)

CONTENTS

1. Synthesis of $Sr_2MGe_2S_6O$ and $Sr_2ZnGe_2O_7$

All highly purified (>99.9%) raw materials (SrS, MO, GeS_2) were purchased from the Beijing Hawk Science & Technology Co., Ltd without futher purification.

$Sr_2MGe_2S_6O$ (M = Zn, Cd) were synthesized by solid-state reaction with SrS, MO and GeS_2 in a 2:1:2 ratio. Raw materials were weighed and mixed in an argon-filled glove box and vacuum-sealed quartz tubes were placed in a temperature-controlled muffle furnace. This furnace was firstly heated to 900 ^oC within 40 h, kept at this temperature for 80 h, and then slowly lowered to room temperature within 100 h. The yield of product crystals is greater than 95% and they are stable in the air. The polycrystalline sample of $Sr_2ZnGe_2O_7$ as reference were also synthesized by the stoichiometric ratio at the sinter temperature at 1000 ^oC within 72 h.

2. Structural Refinement and Crystal Data

Selected high-quality crystals were used for data collections on a Bruker D8 VENTURE diffractometer using Mo Kα radiation (λ = 0.71073 Å) at 296 K. The crystal structures were solved by direct method and refined using the SHELXTL program package. Multi-scan method was used for absorption correction. Rational anisotropic thermal parameters for all atoms were obtained by the anisotropic refinement and extinction correction. Detail refinement parameters and data were shown in Table S1.

3. Property Characterization

3.1 Powder X-ray Diffraction

Powder X-ray diffraction (XRD) patterns of title compounds were collected on a Bruker D2 X-ray diffractometer with Cu Kα radiation (λ = 1.5418 Å) at room temperature. The 2θ range was 10-70° with a step size of 0.02° and a fixed counting time of 1s/step.

3.2 UV−Vis−Near-IR (NIR) Diffuse-Reflectance Spectrum

Diffuse-reflectance spectra were measured by a Shimadzu SolidSpec-3700DUV spectrophotometer in the wavelength range of 200−800 nm at room temperature.

3.3 Thermal analysis

A HCT-2 (HENVEN) thermal analyzer was used to investigate their differential

scanning calorimetric (DSC) curves in vacuum-sealed silica tubes from 30 to 1100 °C. The heating and the cooling rates were 7 °C/min, respectively.

3.4 Second-harmonic Generation Measurement

Through the Kurtz and Perry method, powder SHG response was investigated by a Q-switch laser (2.09 μm, 3 Hz, 50 ns) with different particle sizes, including 38−55, 55−88, 88−105, 105−150, 150−200, and 200−250 μm. The $AgGaS_2$ crystal was ground and sieved into the same size range as the reference.

3.5 Computational Description

The Gaussian 09 package was employed to explore the electronic structures of GeS_3O and GeO_4 anionic groups at molecular level. DFT method at the CAM-B3LYP level with 3-21G basis sets was performed to calculate the cluster.

In order to further investigate the structure–property relationship, electronic structures of $Sr_2MGe_2S_6O$ and $Sr_2ZnGe_2O_7$ was studied by density functional theory calculation. Exchange-correlation potential was calculated using Perdew–Burke–Ernzerhof (PBE) functional within the generalized gradient approximation (GGA) with the scheme. The following orbital electrons were treated as valence electrons, Sr: $4p^6\ 5s^2$, Zn: $3d^{10}\ 4s^2$, Cd: $4d^{10}\ 5s^2$, Ge: $4s^2\ 4p^2$, S: $3s^2\ 3p^4$, O: $2s^2\ 2p^4$. To achieve energy convergence, a plane-wave basis set energy cutoff was 750 eV within normal-conserving pseudo-potential (NCP). As important parameters for NLO crystal, SHG coefficient and refractive index were also calculated. SHG-density in VE and VH process were also calculated to analyze the contribution of anionic groups. Owing to the discontinuity of exchange correlation energy, the experimental value is usually larger than that of calculated band gap. Thus, scissors operator is used to make the conduction band agree with the experimental value.

4. Figures and Tables

Table S1. Crystal data and structure refinement for $Sr_2MGe_2S_6O$.

Table S2. Atomic coordinates and equivalent isotropic displacement parameters of $Sr_2MGe_2S_6O$ (M = Zn, Cd).

Fig. S1 Crystal structures of $Sr_2CdGe_2S_6O$ (left) and $Sr_2ZnGe_2S_6O$ (right).

Fig. S2 Powder XRD patterns of $Sr_2ZnGe_2O_7$.

Fig. S3 Optical bandgap of $Sr_2ZnGe_2O_7$.

Fig. S4 SHG intensity versus particle size in $Sr_2ZnGe_2O_7$.

Fig. S5 Band structure and PDOS diagram of $Sr_2ZnGe_2O_7$.

Fig. S6 Birefringence *versus* wavelength of $Sr_2MGe_2S_6O$ and $Sr_2ZnGe_2O_7$.

Table S1. Crystal data and structure refinement for $Sr_2MGe_2S_6O$ (M = Zn, Cd).

Empirical formula	$Sr_2ZnGe_2S_6O$	$Sr_2CdGe_2S_6O$
formula weight	594.15	641.18
crystal system	*Tetragonal*	*Tetragonal*
space group	$P\bar{4}21m$	$P\bar{4}21m$
cell parameter *a* (Å)	9.4322(6)	9.6080(2)
cell parameter *b* (Å)	9.4322(6)	9.6080(2)
cell parameter *c* (Å)	6.1813(5)	6.2085(2)
Z, *V* (Å^3) (Volume)	2, 549.93(8)	2, 573.13
D_c (g/cm^3) (calculated density)	3.588	3.715
μ (mm^{-1}) (absorption coefficient)	18.273	17.296
goodness-of-fit on F^2	0.862	0.877
R_1, wR_2 ($I > 2\sigma(I)$)[a]	0.0128, 0.0285	0.0100, 0.0231
R_1, wR_2 (all data)	0.0132, 0.0286	0.0102, 0.0232
Flack parameter	0.012(8)	0.012(6)
largest diff. peak and hole (e·Å^{-3})	0.430, –0.293	0.282, –0.320

[a] $R_1 = F_o - F_c / F_o$ and $wR_2 = [w (F_o^2 - F_c^2)^2 / wF_o^4]^{1/2}$ for $F_o^2 > 2\sigma (F_o^2)$

Table S2. Atomic coordinates and equivalent isotropic displacement parameters of $Sr_2MGe_2S_6O$ (M = Zn, Cd).

$Sr_2ZnGe_2S_6O$				
atoms	*x*	*y*	*z*	δ_{iso}
Sr1	0.658392	0.841608	1.00115	0.01342
Ge1	0.372933	0.872933	0.578017	0.01082
Zn1	1	1	1.5	0.01333
S1	0.365382	0.865382	1.231108	0.01592
S2	0.937106	0.823871	1.25437	0.01064
O1	0.5	1	0.697439	0.01409

$Sr_2CdGe_2S_6O$				
atoms	*x*	*y*	*z*	δ_{iso}
Sr1	0.843738	0.343738	0.488479	0.01671
Ge1	0.875708	0.624292	0.904828	0.01488
Cd1	1	0	0	0.01040
S1	0.865836	0.634164	1.250002	0.01918
S2	0.815804	0.062348	0.265971	0.01615
O1	1	0.5	0.789574	0.01703

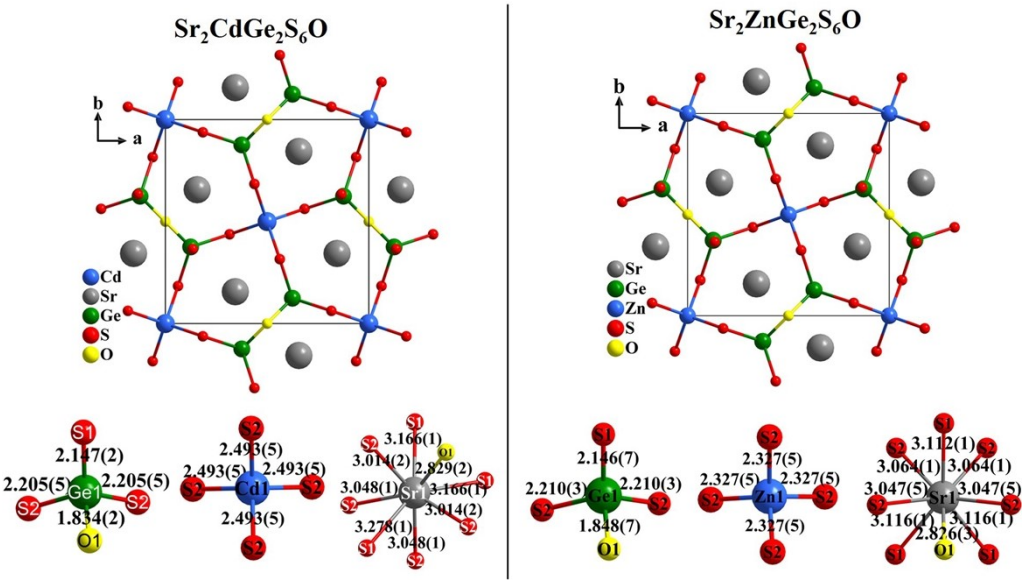

Fig. S1 Crystal structures of $Sr_2CdGe_2S_6O$ (left) and $Sr_2ZnGe_2S_6O$ (right).

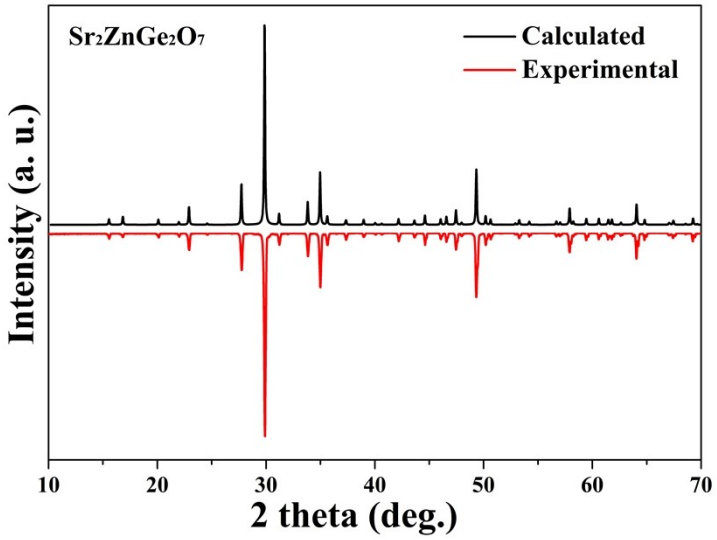

Fig. S2 Powder XRD patterns of $Sr_2ZnGe_2O_7$.

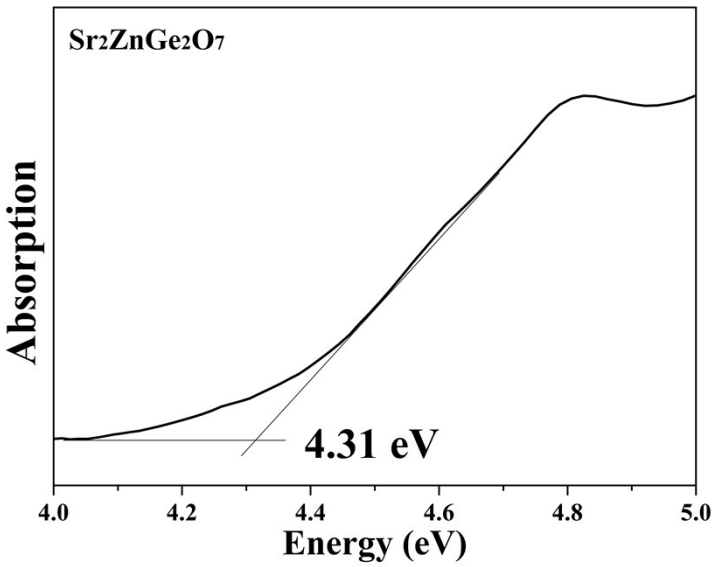

Fig. S3 Optical bandgap of $Sr_2ZnGe_2O_7$.

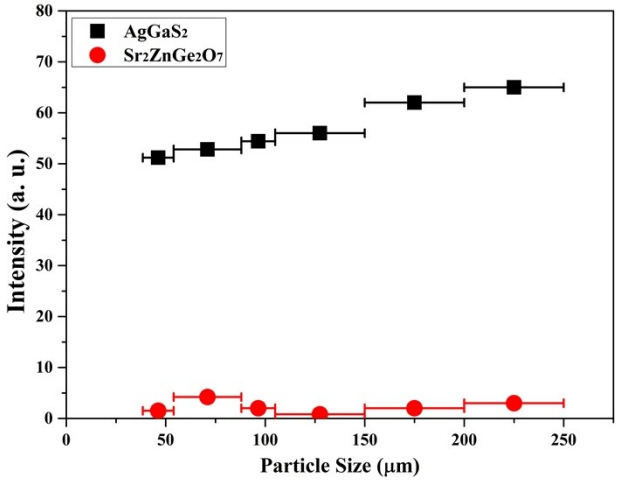

Fig. S4 SHG intensity versus particle size in $Sr_2ZnGe_2O_7$.

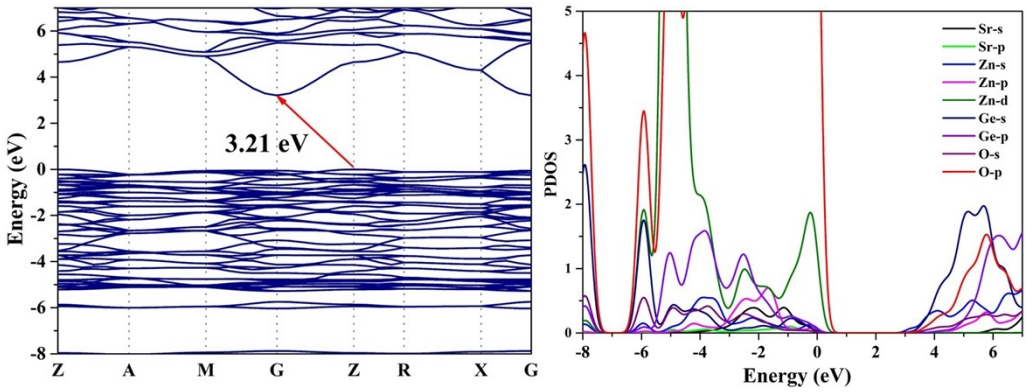

Fig. S5 Band structure and PDOS diagram of $Sr_2ZnGe_2O_7$.

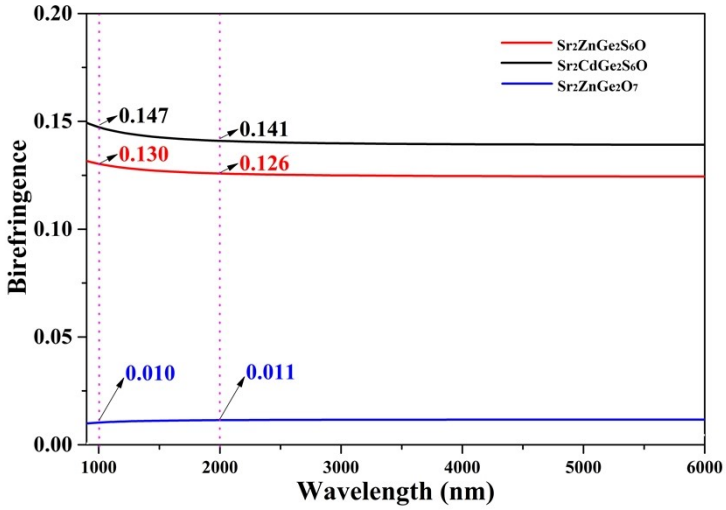

Fig. S6 Birefringence *versus* wavelength of $Sr_2MGe_2S_6O$ and $Sr_2ZnGe_2O_7$.